

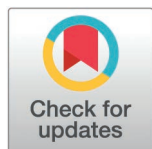
RESEARCH ARTICLE

Understanding disease-associated metabolic changes in human colonic epithelial cells using the *iColonEpithelium* metabolic reconstruction

Boyu Jiang^{1,2}, Nick Quinn-Bohmann³, Christian Diener^{3,4}, Vignesh Bose Nathan⁵, Yu Han-Hallett⁶, Lavanya Reddivari⁵, Sean M. Gibbons^{3,7,8,9,*}, Priyanka Baloni^{1,2,*}

1 School of Health Sciences, Purdue University, West Lafayette, Indiana, United States of America, **2** Purdue Institute for Integrative Neuroscience, Purdue University, West Lafayette, Indiana, United States of America, **3** Institute for Systems Biology, Seattle, Washington, United States of America, **4** Diagnostic and Research Institute of Hygiene, Microbiology and Environmental Medicine, Medical University of Graz, Graz, Austria, **5** Department of Food Science, Purdue University, West Lafayette, Indiana, United States of America, **6** Bindley Bioscience Center, Purdue University, West Lafayette, Indiana, United States of America, **7** Department of Bioengineering, University of Washington, Seattle, Washington, United States of America, **8** Department of Genome Sciences, University of Washington, Seattle, Washington, United States of America, **9** eScience Institute, University of Washington, Seattle, Washington, United States of America

* pbaloni@purdue.edu (PB); sgibbons@isbscience.org (SMG)



OPEN ACCESS

Citation: Jiang B, Quinn-Bohmann N, Diener C, Nathan VB, Han-Hallett Y, Reddivari L, et al. (2025) Understanding disease-associated metabolic changes in human colonic epithelial cells using the *iColonEpithelium* metabolic reconstruction. *PLoS Comput Biol* 21(7): e1013253. <https://doi.org/10.1371/journal.pcbi.1013253>

Editor: Kiran R. Patil, University of Cambridge, UNITED KINGDOM OF GREAT BRITAIN AND NORTHERN IRELAND

Received: November 5, 2024

Accepted: June 17, 2025

Published: July 3, 2025

Copyright: © 2025 Jiang et al. This is an open access article distributed under the terms of the [Creative Commons Attribution License](https://creativecommons.org/licenses/by/4.0/), which permits unrestricted use, distribution, and reproduction in any medium, provided the original author and source are credited.

Data availability statement: The code developed for this study is available at <https://doi.org/10.4231/DNBT-5G17> and <https://github.com/BaloniLab/iColonEpithelium>.

Abstract

The colonic epithelium plays a key role in the host-microbiome interactions, allowing uptake of various nutrients and driving important metabolic processes. To unravel detailed metabolic activities in the human colonic epithelium, our present study focuses on the generation of the first cell-type-specific genome-scale metabolic model (GEM) of human colonic epithelial cells, named *iColonEpithelium*. GEMs are powerful tools for exploring reactions and metabolites at the systems level and predicting the flux distributions at steady state. Our cell-type-specific *iColonEpithelium* metabolic reconstruction captures genes specifically expressed in the human colonic epithelial cells. *iColonEpithelium* is also capable of performing metabolic tasks specific to the colonic epithelium. A unique transport reaction compartment has been included to allow for the simulation of metabolic interactions with the gut microbiome. We used *iColonEpithelium* to identify metabolic signatures associated with inflammatory bowel disease. We used single-cell RNA sequencing data from Crohn's Diseases (CD) and ulcerative colitis (UC) samples to build disease-specific *iColonEpithelium* metabolic networks in order to predict metabolic signatures of colonocytes in both healthy and disease states. We identified reactions in nucleotide interconversion, fatty acid synthesis and tryptophan metabolism were differentially regulated in CD and UC conditions, relative to healthy control, which were in accordance with experimental results. The *iColonEpithelium* metabolic network can be used to identify mechanisms at the cellular level, and we show an initial proof-of-concept for how our tool can be leveraged to explore the metabolic interactions between host and gut microbiota.

Funding: Research reported in this publication was supported by the National Institute of Diabetes and Digestive and Kidney Diseases of the National Institutes of Health under award number R01DK133468 (to S.M.G.) The funders did not play any role in the study design, data collection and analysis, decision to publish, or preparation of the manuscript.

Competing interests: We have read the journal's policy and the author of this manuscript have the following competing interests: S.M.G. is a paid member of the Thorne Scientific Advisory Board. This role is entirely unrelated to the research reported in this manuscript.

Author summary

The human colonic epithelium mediates nutrient absorption and participates in extensive metabolic interactions with the gut microbiota. To better understand the metabolic functions of colonic epithelial cells, we developed iColonEpithelium, the first cell-type-specific genome-scale metabolic model (GEM) of human colonocytes. GEMs are computational frameworks that simulate how genes and metabolites interact within a cell's metabolic network. We show the application of iColonEpithelium in predicting metabolic alterations in inflammatory bowel disease (IBD) by integrating single-cell RNA sequencing data from IBD patients into the model. Our analysis revealed distinct differences in nucleotide interconversion, fatty acid synthesis, and tryptophan metabolism between healthy and diseased states, consistent with experimental findings. We also incorporated a transport reaction compartment to simulate metabolic interactions with the gut microbiota, paving the way for studying host-microbiome co-metabolism. This study provides a novel computational resource for systems-level analysis of intestinal metabolism and offers a platform to explore disease mechanisms and potential therapeutic targets in IBD and other digestive disorders.

Introduction

The human colon plays an important role in the host metabolism, coordinating dietary nutrient absorption and interactions with the colonic microbiota [1]. The colonic epithelium serves as a barrier and helps to regulate mucosal and systemic immunity, physiology, and metabolism, mediated in part by interactions with the gut microbiota [2]. Studies have indicated that a compromised colonic epithelium is associated with intestinal diseases, including inflammatory bowel disease (IBD), systemic disorders such as type 1 diabetes, and neurological disorders [3–5]. These studies primarily focused on intestinal permeability and intestinal barrier integrity. Tight junction proteins expressed by colonocytes, including occludin, claudins, and zonula occludins, are important for normal barrier function and are regulated by many factors such as diet, pathogens, and environmental stress [6].

In addition to its role as a physical barrier, recent studies have highlighted metabolic functions of colonic epithelial cells. For example, oxygen consumption by colonocytes, driven by mitochondrial β -oxidation of short-chain fatty acids (SCFAs), helps to maintain anaerobic conditions in the gut lumen and thus shapes the ecology of the gut microbiome [7]. Lactate produced from colonocytes can affect the composition of the gut microbiota during gut inflammation [8]. Metabolic circuits between colonic epithelium and the gut microbiome can potentially influence the blood metabolome [9,10]. Apart from interacting with the gut microbiome, colonic epithelial cells can also affect immune cell functions through specific metabolic circuits. For instance, arginine and tryptophan, catabolized in colonic epithelial cells, were reported to have immunoregulatory effects in many diseases [10]. Therefore, exploring the metabolic network

of colonocytes in healthy and disease and their relationships with the gut microbiota is a promising avenue towards identifying microbiome-mediated therapeutic strategies.

Due to the complexity of the metabolic interactions between colon epithelium and the gut microbiota, computational tools such as genome-scale metabolic modeling are required, which can improve both comprehensiveness and specificity of such interactions. Genome-scale metabolic models (GEMs) are network-based tools representing biochemical information in a mathematical format. These *in silico* reconstructions can integrate transcriptome, metabolome, and other omics data [11,12] and enable us to simulate and predict metabolic fluxes through these reaction networks [13,14]. GEMs of the gut microbiome and the human tissues have been repeatedly applied in studies of host-microbiome interactions to facilitate the exploration of the mechanisms underlying metabolic disorders and the development of potential dietary interventions [15–18].

To obtain more insights into the metabolic activities of the human colonic epithelium, we present a cell-type-specific GEM of human colonic epithelial cells, called iColonEpithelium. iColonEpithelium can achieve essential metabolic functions of the human colonic epithelium and enables exploration of the metabolic changes in the cells across diverse conditions. The reconstruction has been made context- or condition-specific by integration of transcriptome and metabolome data to study the underlying mechanisms involved in various health-related outcomes. By defining specific transport reactions for co-metabolites that can pass between colonic epithelial cells and the gut microbiota, and adding them to iColonEpithelium, we show a proof-of-concept for how this model can be leveraged to simulate interactions between the gut epithelium and the gut microbiota.

Results

Metabolic reconstruction of human colonic epithelial cells: iColonEpithelium

We generated the first human colonic epithelial cell-type-specific metabolic network using the generic human reconstruction, Recon3D [19], as the template (see Methods). iColonEpithelium metabolic reconstruction has 6651 reactions, 4072 metabolites, and 1954 genes (Tables A, B, and C in [S1 Data](#)). We used transcriptome data of colonic epithelial cells from healthy individuals to build the reconstruction (Table D in [S1 Data](#)). We obtained draft reconstructions using four established tools for generating context-specific metabolic reconstructions (see Methods section). Metabolites and reactions from all four drafts were compared and combined into a consensus reconstruction, that was finally refined for the generation of iColonEpithelium reconstruction. We compared iColonEpithelium reconstruction with the generic colon organ reconstruction, published as part of the human whole-body model [17]. Since our reconstruction was generated with transcriptomics data from the colonic epithelium, it primarily reflected metabolic features specific to colonocytes instead of the whole colon. For example, our reconstruction contained the reaction of mitochondrial acetate metabolism, which is catalyzed by acetyl-CoA synthetase. This reaction is not included in the colon part of the human whole-body model but can contribute to a better understanding of mitochondrial energy metabolism of colonocytes. Furthermore, objective functions of the iColonEpithelium were decided based on the metabolic function of colonocytes, which put more emphasis on short chain fatty acid (SCFA) metabolism. As shown in [Fig 1](#), we found that approximately 37% of reactions in our reconstruction overlapped with reactions in the colon part of the whole-body model and 95% of reactions in our reconstruction overlapped with reactions in Recon3D. The percentages of the overlapping metabolites and genes in the iColonEpithelium with the colon reconstruction were about 44% and 86%, respectively; while in comparison with Recon3D, our reconstruction shared 96% metabolites, and all its genes overlapped with Recon3D (details in [Fig 1](#)). Moreover, subsystems in the iColonEpithelium (Table E in [S1 Data](#)) covered 103 metabolic pathways and the distribution of subsystems demonstrated that the top 10 most frequent subsystems belonged to transport reactions, fatty acid metabolism and lipid metabolism ([Table 1](#)), which suggests important metabolic functions of colonocytes involve exchanges and utilization of lipids, especially fatty acids [10,20]. Because previous studies have emphasized that beta-oxidation of SCFAs plays an important role in the physiological function of human colonic epithelial cells [7], we used biomass maintenance and SCFA production as the objective functions in our reconstruction.

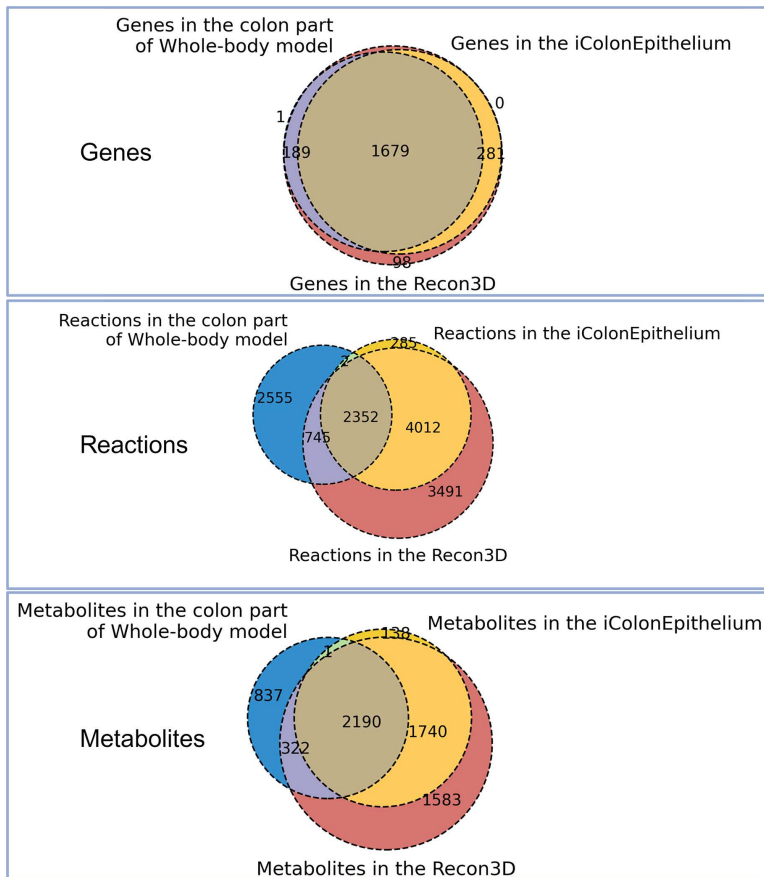


Fig 1. Venn diagrams indicating the overlap of genes, reactions and metabolites between iColonEpithelium, Recon3D and colon part of Whole-body model (Harvey and Harvetta).

<https://doi.org/10.1371/journal.pcbi.1013253.g001>

Table 1. Distribution of top 10 subsystems in the iColonEpithelium.

Subsystem	Frequency
Transport, extracellular	1482
Fatty acid oxidation	857
Extracellular exchange	715
Transport, mitochondrial	275
Cholesterol metabolism	234
Fatty acid synthesis	228
Glycerophospholipid metabolism	140
Nucleotide interconversion	137
Transport, lumen	137
Lumen exchange	137

<https://doi.org/10.1371/journal.pcbi.1013253.t001>

As a next step to assess the specificity of our reconstruction, we tested the iColonEpithelium reconstruction's ability to achieve specific metabolic tasks. A total of 229 metabolic tasks associated with basic mammalian cells or human colonic epithelial cells were identified from published literature (Table F in [S1 Data](#)). The consensus reconstruction passed ~84% of them, including the β -oxidation of butyrate and acetate to generate ATP [7], and the synthesis of cholesterol and spermidine [21,22], which were reported as important metabolic functions for colonocytes. These refinement steps suggested that the iColonEpithelium reconstruction is cell-type-specific and can be used for predicting the metabolic functions of the colonic epithelium.

Identification of transport reactions to enable connections between colonic epithelial cells and gut microbiota

To enable iColonEpithelium reconstruction to interact with the gut microbiota, we collected information regarding transport reactions and added them to the reconstruction. We used the information from the Human Protein Atlas (<https://www.proteinatlas.org>) [23] and 624 of these genes (Table G in [S1 Data](#)) mapped to the reconstruction. We mined the information of the metabolic reactions corresponding to mapped genes from the Uniprot (<https://www.uniprot.org>) and Rhea (<https://www.rhea-db.org>) databases [24,25], which provided us with 247 metabolites involved in the transport reactions. Information regarding transport reactions and corresponding metabolites from a published transport module [26] and the colon part of the whole-body model [17] were also extracted and used for reconstruction. After comparing all metabolites and checking their transport in the EMBL database (<https://www.embl.org>) [27], we settled on 139 metabolites that connect the reconstruction to the gut microbiota in the colon lumen, including SCFAs and bile acids (Table H in [S1 Data](#)). We assigned these metabolites to the 'lumen' compartment and their corresponding transport reactions were added to the reconstruction. With the lumen compartment and curated transport reactions, the iColonEpithelium reconstruction is able to simulate metabolic activities of colonic epithelial cells interacting with the gut microbiota.

Metabolomic profiling and validation of iColonEpithelium using Caco-2 cell culture

We carried out *in vitro* culturing of colon carcinoma cell line (Caco-2) and performed targeted metabolomics to quantify concentrations of specific metabolites, such as amino acids and SCFAs in the cell culture medium. Since Caco-2 cells have been widely used as an *in vitro* model to study the function and metabolism of intestinal epithelium [28], the changes of metabolite concentrations in the medium can reflect the capacity of colonocytes in utilizing or producing specific metabolites. We cultured Caco-2 cells with Dulbecco's Modified Eagle Medium (DMEM) supplemented with fetal bovine serum (FBS) for 2 days and performed targeted metabolomics analysis of 20 amino acids. The cells mainly consumed 7 amino acids (glutamine, glutamate, isoleucine, leucine, phenylalanine, serine and valine) from the medium, while proline was secreted into the medium (Table 2). Previous reports have shown increased production of proline in Caco-2 cells [29]. The concentration of acetate in the cell culture medium decreased by 54%, compared with original medium (Table 2). It has been demonstrated that colonic epithelial cells could utilize acetate from the extracellular environment, which is in accordance with reported studies [30], and the iColonEpithelium also contained necessary reactions which allowed uptake of acetate for ATP generation. SCFAs were not specifically added to the DMEM, but their presence in the medium can be attributed to the fetal bovine serum (FBS), as it has been reported that FBS contains various fatty acid components [31].

To determine if the iColonEpithelium was able to predict the uptake or secretion of metabolites observed in the Caco-2 cell culturing experiment, we performed flux variability analysis (FVA) on the metabolic reconstruction. FVA is a technique used to determine the range of possible fluxes through reactions in a GEM, providing insights into flexibility of the network [32]. Based on our FVA results, we identified reactions, especially exchange reactions, that are required by our reconstruction to import or secrete metabolites from or to the extracellular environment, like the culture medium, blood, or the gut lumen. If the minimum flux of an exchange reaction in a GEM is negative, this represents uptake from the extracellular environment, namely the medium, into the intracellular space; similarly, if the maximum flux of an exchange reaction in a

GEM is positive value, this metabolite is secreted from the intracellular space to the extracellular environment. By simulating the uptake of metabolites from DMEM medium in our reconstruction (Table 2) and then running FVA, we found that the iColonEpithelium was able to uptake the 7 amino acids mentioned above, as well as synthesize proline with the DMEM, which is concurrent with our empirical observations.

The above validation checks [19] for the iColonEpithelium confirmed that it passes some basic requirements, like containing no leaks in the reconstruction, generating no ATP from water, and maintaining flux consistency (Table I in S1 Data). The reconstruction was also queried in the Memote tool [33], which ensured the quality of iColonEpithelium (S2 Data). The results of these checks are provided in Table I in S1 Data.

Identifying the metabolic signatures in ulcerative colitis and Crohn’s disease using iColonEpithelium reconstruction

Generate context-specific reconstructions from single-cell RNA sequencing data. We used single-cell RNA sequencing (scRNAseq) data from patient samples to constrain the iColonEpithelium reconstruction to investigate metabolic changes in two types of inflammatory bowel diseases (IBD): Crohn’s disease (CD) [34] and ulcerative colitis (UC) [35]. The CD study consisted of transcriptome data of colonocytes from 4 healthy and 3 CD samples and we

Table 2. Targeted metabolomic analysis on metabolites from Caco-2 cells culturing medium.

Metabolites	Cell Culture Medium (ng/uL)	DMEM+ FBS (ng/uL)	Range of Exchange reaction fluxes
Butyrate	0.04 ± 0.005	0.06	(-1.0, 0.0)
Acetate*	8.49 ± 0.56	18.43	(-1.0, 42.15)
Propionate	3.45 ± 2.48	17.02	(-1.0, 24.50)
Alanine	116.28 ± 42.90	12.55	(-1.0, 21.03)
Arginine	53.93 ± 26.74	110.89	(-1.0, 5.56)
Cysteine	0.13 ± 0.05	0.02	(-1.0, 2.0)
Glutamine*	62.10 ± 26.86	172.48	(-1.0, 10.13)
Glutamate*	1.31 ± 0.49	8.15	(-1.0, 16.60)
Histidine	54.82 ± 24.94	43.28	(-1.0, 0.0)
Isoleucine*	91.51 ± 35.18	214.70	(-1.0, 0.0)
Leucine*	55.22 ± 26.04	176.23	(-1.0, 0.0)
Lysine	110.97 ± 27.42	160.63	(-1.0, 0.0)
Methionine	47.36 ± 24.04	91.39	(-1.0, 0.0)
Phenylalanine*	1724.69 ± 3372.22	3372.22	(-1.0, 0.0)
Proline*	40.61 ± 10.18	7.80	(-1.0, 16.78)
Serine*	20.23 ± 8.55	42.08	(-1.0, 8.97)
Threonine	34.82 ± 11.13	54.92	(-1.0, 0.0)
Asparagine	1.93 ± 0.20	NA	(-1.0, 10.12)
Tryptophan	12.43 ± 6.71	22.94	(-1.0, 0.0)
Tyrosine	329.51 ± 172.40	667.66	(-1.0, 1.0)
Valine*	115.72 ± 50.06	260.68	(-1.0, 0.0)
Glycine	28.90 ± 9.68	20.84	(-1.0, 18.74)

Metabolites marked with *represented their concentration changes in the cell culture medium have statistical significance (Student’s t-test, p-value < 0.05) compared to the DMEM medium + FBS. Negative values mean that the reconstruction can uptake corresponding metabolites from the extracellular medium, while positive values mean that the model can synthesize and secrete corresponding metabolites to the extracellular medium.

<https://doi.org/10.1371/journal.pcbi.1013253.t002>

generated context-specific metabolic networks for each sample in this study using the iMAT algorithm [36]. Similarly for the UC study, we generated 36 context-specific reconstructions from 23 healthy samples and 13 UC samples.

Understanding the metabolic differences in CD and UC cases. To explore metabolic differences in CD and UC conditions, we performed flux variability analysis on the context-specific metabolic reconstructions. We calculated minimum and maximum fluxes of reactions in each context-specific reconstruction. We compared the maximum reaction fluxes between the healthy and IBD samples in the CD and UC studies and carried out statistical analysis to identify reactions with significant flux differences. In the CD study, we identified 12 reactions whose maximum fluxes are significantly different with respect to the healthy controls. These reactions were mainly associated with fatty acid metabolism, keratan sulfate degradation and creatine uptake (Table 3a). In the UC study we identified 22 reactions

Table 3. Comparison of reaction maximum fluxes between inflammatory and healthy groups in CD and UC, respectively. A: CD study: Different maximum fluxes between healthy and inflammatory groups. B: UC study: Different maximum fluxes between healthy and inflammatory groups.

A		
Reaction	Subsystem	p-value (Student's t-test)
Transport_creat_lu	Transport, lumen	0.01772
EX_arg__L_e	Extracellular exchange	0.01772
SK_arg__L_c	Intracellular source/sink	0.03419
HMR_2193	Fatty acid synthesis	0.03642
HMR_2265	Fatty acid synthesis	0.03743
HMR_3433	Fatty acid oxidation	0.03878
CDSm	Glycerophospholipid metabolism	0.03878
NDPK3m	Nucleotide interconversion	0.03878
PA_HStm	Transport, mitochondrial	0.04156
NAGA2ly	Keratan sulfate degradation	0.04645
B		
Reaction	Subsystem	p-value (Student's t-test)
EX_dgchol_e	Extracellular exchange	1.85113E-05
UGALNACtg	Transport, golgi apparatus	2.47163E-05
SO4tl	Transport, lysosomal	0.00096
PAPtg	Transport, golgi apparatus	0.00222
NACHEX25ly	Keratan sulfate degradation	0.00345
IDPt_n	Transport, nuclear	0.00462
DIDPt_n	Transport, nuclear	0.00462
NDPK9n	Nucleotide interconversion	0.00462
NDPK10n	Nucleotide interconversion	0.00462
r0611	Miscellaneous	0.00462
UDPt_l	Transport, lysosomal	0.00488
GLCNACASE4ly	Heparan sulfate degradation	0.00590
ELAIDCRNt	Fatty acid oxidation	0.00974
UAGDP	Aminosugar metabolism	0.01320
LDH_D	Pyruvate metabolism	0.01363
ALAR	Alanine and aspartate metabolism	0.01440
RE3273C_1	Phosphatidylinositol phosphate metabolism	0.01578
Transport_cmp_lu	Transport, lumen	0.03249

<https://doi.org/10.1371/journal.pcbi.1013253.t003>

with significant flux differences between healthy and UC groups that were part of nucleotide metabolism and metabolite transportation (Table 3b).

Additionally, we carried out Monte Carlo Artificially Centered Hit and Run (ACHR) flux sampling to evaluate flux distributions belonging to tryptophan metabolism and nucleotide interconversion from the context-specific reconstructions. Flux sampling allowed us to perform an unbiased assessment of all possible flux distributions in the solution space of each context-specific reconstruction. For tryptophan metabolism, we identified that UC colonocytes showed lower flux distribution for the reaction that deaminates serotonin into 5-Hydroxyindoleacetaldehyde (5HOXINOXDA) (Fig 2A). CD colonocytes showed similar flux distributions for this particular reaction compared to healthy colonocytes. CD colonocytes showed higher fluxes in the conversion of acetoacetyl-CoA to crotonoyl-CoA (HACD1m and ECOAH1m), while these fluxes did not vary significantly between UC and healthy colonocytes. UC and healthy colonocytes had similar flux distributions for nucleotide interconversion among ATP, GDP, UDP, CDP and IDP, while CD colonocytes showed more variation in nucleotide interconversion when compared to healthy colonocytes (Fig 2B).

In silico gene knockout simulations identify metabolic pathways affected in UC and CD. GEMs contain information on gene-protein-reaction (GPR) associations in the system that is useful for integration of multi-omics data. We can perform *in silico* single gene knockout to predict essential genes in the reconstruction as well as identify the effects of genes in the system. For the present case study, we performed *in silico* single-gene knockout simulation on all

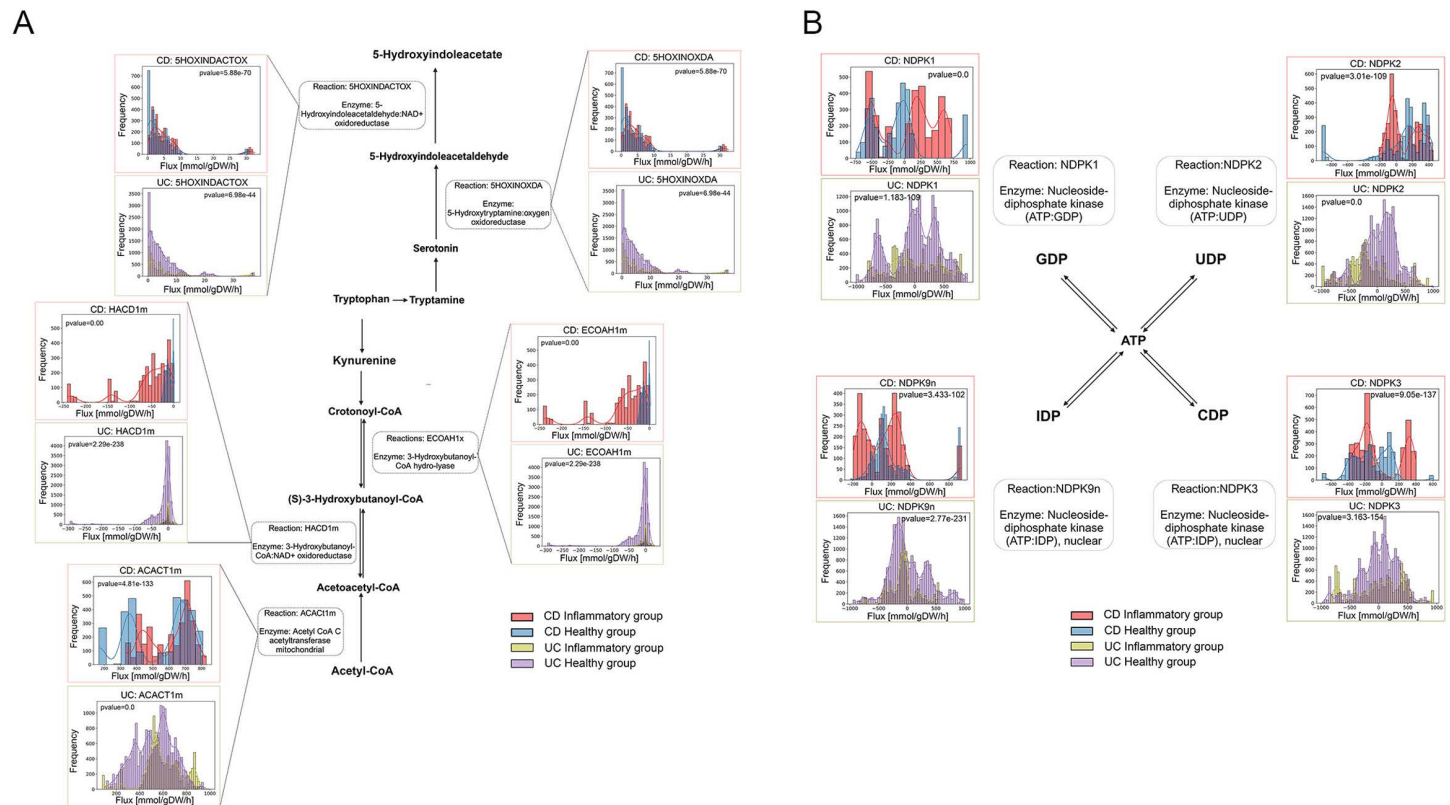


Fig 2. A) Bar plots indicating the comparison of flux distributions in tryptophan metabolism pathways between inflammatory and healthy group colonocytes from CD and UC, respectively. P-values were calculated with Kolmogorov-Smirnov test, reactions in the figure are the BIGG reaction ID; **B)** Bar plots indicating the comparison of flux distributions in nucleotide interconversion pathways between inflammatory and healthy group colonocytes from CD and UC, respectively. P-values were calculated with Kolmogorov-Smirnov test, reactions in the figure are the BIGG reaction ID.

<https://doi.org/10.1371/journal.pcbi.1013253.g002>

context-specific metabolic reconstructions in both CD and UC studies and compared the output of the biomass objective function. Changes in metabolic fluxes within biomass objective function could represent changes in cell viability [19]. The result of knockout simulations in CD colonocytes predicted that genes associated with glyoxylate and dicarboxylate metabolism (*GRHPR*), cholesterol metabolism (*HMGCS2*), CoA synthesis (*PPCS*), and transportation of metabolites (*SLC5A11* and *SLC5A7*) had significant effects on viability (Fig 3A). In the UC colonocytes, single gene knockouts that significantly affected the biomass objective function were associated with carnitine metabolism (*CRAT*), glyoxylate and dicarboxylate metabolism (*ALDH9A1*) and transportation of metabolites (*SLC4A7*, *CRAT* and *CFTR*) (Fig 3B). This suggests the importance of several pathways in the context of IBD, like glyoxylate and dicarboxylate metabolism, as this pathway could affect objective functions of CD and UC reconstructions. Similar observations have also been reported in a study employing gut microbiome GEMs, which showed associations among glyoxylate and dicarboxylate metabolism, metabolic disorders and inflammation [37].

Comparing effects of gene knockouts between the IBD and healthy control groups showed that these genes played different roles in the maintenance of the biomass objective function. *PCYT2* gene knockouts were shown to cause a greater decrease in the objective function of CD colonocytes than healthy colonocytes. Knockouts of 5 genes (*PPCS*, *HMGCS2*, *GRHPR*, *SLC5A11* and *SLC5A7*) were predicted to cause a greater decrease in the objective function in CD colonocytes than healthy colonocytes. Compared to CD, we identified additional genes (*SLC4A7*, *CRAT* and *CFTR*) predicted to have a greater effect on decreasing flux of objective function in UC colonocytes. The gene knockout simulations reveal key metabolic pathways and transport mechanisms that significantly influence cell viability in IBD conditions. The differential effects of specific genes between CD and UC colonocytes, as well as between IBD and healthy controls, underscore the importance of pathway-specific interventions.

Capturing metabolite exchanges between the gut microbiota and human colonocytes

To demonstrate application of iColonEpithelium reconstruction in the context of host-microbiome interactions, we integrated our metabolic network with a community-scale metabolic modeling platform, called MICOM, which can be used to build individual-specific models of commensal gut microbiota [38]. The goal of this analysis was to illustrate metabolic exchanges between the host and the gut microbiota. The integrated model showed that iColonEpithelium and all 35

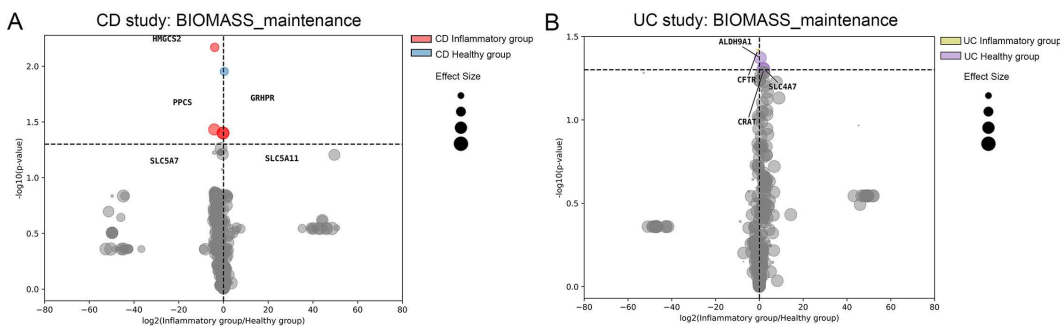


Fig 3. A) Volcano plot comparing effects of single gene knockout simulations on the colonocyte BIOMASS_maintenance flux between inflammatory and healthy group colonocytes from CD. X-axis: $\log_2(\text{Inflammatory group/Healthy group})$, where “Inflammatory group” represents the mean (WT-KO)/WT ratio in colonocytes of inflammatory group, and “Healthy group” equals the mean (WT-KO)/WT ratio in colonocytes of healthy group; values <0 (colored dot on the left of the vertical dotted line) signify knockouts with greater effects on BIOMASS_maintenance in colonocytes of inflammatory group, whereas values >0 (colored dot on the right of the vertical dotted line) signify knockouts with greater effects on BIOMASS_maintenance in colonocytes of healthy group. Y-axis: statistical significance (p-values calculated by student’s t-test) comparing knockout effects between inflammatory and healthy groups; dots above the horizontal dotted line (t-test p-value ≤ 0.05) are statistically significant. The size of each dot is proportional to the overall effect size (mean (WT-KO)/WT ratio across all inflammatory and healthy groups).; B) Comparison of effects of single gene knockout simulations on the colonocyte BIOMASS_maintenance flux between inflammatory and healthy group colonocytes from UC.

<https://doi.org/10.1371/journal.pcbi.1013253.g003>

microbial genera in the MICOM model were able to achieve feasible biomass maintenance and growth (Table J in [S1 Data](#)). In the MICOM model used in this analysis, *Phocaeicola*, an anaerobic gram-negative genus commonly found in the human gut, showed the highest abundance and growth rate. The MICOM model contributed much more towards the production of SCFAs, such as butyrate, acetate and propionate, than consumption of these metabolites (Table K in [S1 Data](#)). We identified 35 metabolites, including lactate, bicarbonate, and guanosine monophosphate (GMP), that were secreted by the iColonEpithelium and taken up by the MICOM model (Table L in [S1 Data](#)). Additionally, we observed that the iColonEpithelium reconstruction took up 88 metabolites from the MICOM model, including formate, acetate, succinate and citrate (Table L in [S1 Data](#)). 57.5% of the butyrate and 61.5% of the acetate produced by the MICOM model were taken up by the iColonEpithelium part, with the absolute flux values as 0.003838 and 0.254941 mol/ [1 gDW * Day], respectively.

Discussion

In this study, we present a metabolic reconstruction of human colonic epithelial cells, iColonEpithelium, which is useful for predicting metabolic phenotypes in the gut epithelium at the cellular level. The following are the key features of this cell-specific reconstruction: a) this is the first reported cell-type-specific metabolic reconstruction of human colonic epithelial cells built from transcriptomics data of clinical biopsies; b) colonic epithelial cells are known to interact with the gut microbiome, so we added a unique compartment named 'lumen' to enable simulation of metabolite exchanges between colonic epithelial cells and the gut microbiome; c) the iColonEpithelium reconstruction was able to simulate the transport of metabolites from the gut microbiome environment, as well as transport of metabolites into the portal vein; d) the reconstruction achieved cell-type specificity based on successful completion of several metabolic tasks important for colonic epithelial cells; e) through the integration of patient-derived single cell transcriptomic data with metabolic reconstruction, we identified metabolic alterations in ulcerative colitis (UC) and Crohn's disease (CD), highlighting the utility of this *in silico* metabolic reconstruction.

The human colonic epithelium consists of multiple cell types, including colonocytes, goblet cells, enteroendocrine cells, tuft cells, and other immune cells. Compared to other cell types in the colonic epithelium, the colonocytes are the most abundant cell type and take a central role in nutrient exchanges with the gut microbiota and dietary substrates [39]. Recent studies have highlighted the importance of colonocytes in modulating host-microbiota metabolic interactions. For instance, colonocytes are the tissue interface where SCFAs are absorbed and consumed by the host. The consumption of SCFAs, like butyrate and acetate, by colonocytes will affect the availability of these SCFAs for the rest of the body, and β -oxidation of SCFAs in colonocytes is accompanied by a high demand for oxygen, which has a direct effect on maintaining the anaerobic environment within the colon [7]. However, heterogeneous uptakes of SCFAs by colonocytes under different conditions, like changed diet patterns or progression of gastrointestinal diseases, still remain unknown. Studies have indicated strong interactions among the gut microbiota, SCFA production, and colonocyte metabolism [40]. A high-quality colonocyte-specific metabolic model has the potential to provide deeper insights into host-microbiome interactions in the gut.

To ensure the cell-type specificity of the iColonEpithelium reconstruction, the draft reconstruction was initially built with publicly available transcriptomics data of human colon epithelium biopsy samples, consisting largely of colonic epithelial cells. During the refinement and test of our draft reconstruction, we used metabolic tasks that have been reported for human colonic epithelial cells to validate that iColonEpithelium could carry out metabolic functions in accordance with reported experimental studies on the colonocytes. We also employed targeted metabolomics analysis of differentiated Caco-2 cells to determine the utilization of specific metabolites and used these results to refine the iColonEpithelium to make sure that it can capture metabolic functions specific to colonic epithelial cells.

In this study, we also integrated the scRNAseq data of colonocytes from two studies of CD and UC with iColonEpithelium to explore and compare metabolic changes in IBD. It has been reported that IBD is accompanied by metabolic dysfunctions in colonic epithelial cells [10]. Our reconstruction could differentiate metabolic changes in CD and UC

colonocytes, relative to healthy controls. For instance, in the CD, we predicted alterations in fatty acid metabolism, and recent studies have highlighted the importance of long chain fatty acids (LCFAs) in the CD [41]. For the UC, we saw disruptions in nucleotide metabolism, which were catalyzed by nucleoside-diphosphate kinase (*NDPK*) genes. The downregulation of *NDPK* in UC has also been reported previously [42]. Both LCFAs and nucleotide metabolism were correlated with inflammation, which may provide insight into the different mechanisms underlying CD and UC.

We found different patterns in tryptophan metabolism between CD and UC. Tryptophan is an essential amino acid from the diet and its metabolism in the body is mediated by both the gut microbiota and colonic epithelial cells [43]. According to the results (Fig 2A), CD colonocytes showed an increased flux distribution in reactions that degraded serotonin into 5-hydroxyindoleacetate (5-HIAA). It has been reported that the concentration of 5-HIAA from the urine samples of CD patients, which were collected in the afternoon, was higher than the afternoon urine from healthy individuals [44]. We also identified a significant increase of nicotinamide adenine dinucleotide (NAD⁺) production from (S)-3-Hydroxybutanoyl-CoA (Fig 2A, reaction: HACD1m) in the colonocytes from CD patients when compared to colonocytes from healthy individuals. Tryptophan is an import precursor to NAD⁺ production, which serves as a cofactor and participates in a wide range of homeostatic processes. In IBD, dysregulated NAD homeostasis will not only compromise the intestinal barrier but also perturb mucosal immunity [45]. From the analysis in this study, we also highlight the importance of metabolic flux in HACD1m in CD colonocytes.

Single gene knockout simulation allowed us to explore essentiality of genes between CD and UC colonocytes, and some of the predicted essential genes are in accordance with experimental results. For example, a study of *in vitro* model of CD reported upregulated expression levels of *GRHPR*, and knock-down of *GRHPR* could increase apoptosis of intestinal epithelial cells [46]. This validation further substantiates the capacity of our reconstruction to capture important metabolic processes in colonocytes, when combined with -omics data.

We provide proof-of-concept highlighting the integration of our iColonEpithelium reconstruction and the MICOM modeling platform, showing the potential for predicting metabolite exchanges between the host and the gut microbiota. The integrated model could achieve both biomass maintenance of the colonocytes and the growth of all the gut bacterial genera present in the system. The integrated MICOM model achieved microbiota-driven SCFA production [7]. For the colonic model, we observed secretion of metabolites like lactate [8] and bicarbonate [47] to the microbiota, which aligns well with prior isotopic labeling results in mice, showing that these metabolites can flow from the blood into the gut lumen [48]. The iColonEpithelium colonocytes consumed both acetate and butyrate, as expected [49]. Overall, we find evidence for the utility of combining the iColonEpithelium with MICOM to explore host-microbiome metabolic interactions.

In summary, we constructed the first cell-type-specific GEM of human colonic epithelial cells to simulate and explore their metabolic activities. The iColonEpithelium has the capacity to achieve essential metabolic functions of human colonic epithelial cells. When constrained with scRNAseq data from IBD patients, it could predict and capture some important metabolic changes in CD and UC, like fatty acid metabolism and tryptophan metabolism, which were in accordance with experimental results reported in literature [43–45]. The iColonEpithelium appears to be useful in understanding how disease states impact colonic metabolism. Finally, the integration of our colonic epithelial model with community-scale metabolic models of the commensal gut microbiota will enable further exploration of dietary and microbiome effects on host metabolism in healthy and disease states.

Limitations of the study

We recognize that our work has certain limitations. Our *in silico* metabolic reconstruction was built from existing transcriptomic data of human colon epithelium, which contains comprehensive information of genes expressed in a given cell type. We need more data to add other constraints, like enzyme kinetics and thermodynamic parameters. Our current predictions are all assuming the steady state condition. Dynamic simulation requires the estimation of unknown parameters, like the rate constants of reactions, and the validation of these estimated parameters requires time-course experimental

measurements [50]. Unfortunately, these measurements are not available for human colonocytes. For the case studies, we were able to obtain only scRNAseq data from CD and UC samples. There are no human colonocyte studies with matched metabolomics, proteomics and transcriptomics data, which could be used to further constrain our models. Also, there is limited information on the metabolites in the extracellular space available to the colonocytes. Future work should integrate proteomics data from colonocytes to further constraint the GPR parameters. Availability of metabolomics data from both gut microbiota and blood can be helpful in constraining the reconstructions and validate the predictions.

Methods

Collection of transcriptome data and cross-platform normalization

We searched NCBI's GEO database (<https://www.ncbi.nlm.nih.gov/geo/>) and collected transcriptome data of human colonic epithelial cell from published studies with the following criteria: (1) clear description of sample sources, which were from human colon epithelium; (2) inclusion of samples from healthy volunteers; (3) availability of raw data; (4) data published within the last 10 years. As we collected both RNA-seq and microarray data from various platforms based on the above-mentioned criteria, we further applied a recently published tool – Shambala-2 [51] to perform cross-platform normalization. According to the workflow of Shambala-2, we normalized all RNA-seq and microarray raw data separately and then combined them together. The datasets included in the present study are described in details in Table D in [S1 Data](#).

Preparations of inputs for different GEM reconstruction tools and pruning draft reconstructions

We used four prominent reconstruction extraction tools to obtain draft reconstructions for colonocyte, using Recon3D [19] as the template reconstruction. Each of them uses a different algorithm and has different requirements for inputs. The output draft reconstructions from each method were compared and analyzed to ensure comprehensiveness and specificity of our colonic epithelial cell reconstruction. The four methods for generating cell-specific reconstruction are described below:

pymCADRE: *pymCADRE* (v1.2.3, <https://github.com/draeger-lab/pymCADRE/>) is the python version of the *mCADRE* [52]. We first calculated the ubiquity score of genes. After comparing different quantiles of gene values, we used the 30th percentile expression value as the cutoff for gene expression. Then all gene values are binarized according to the cutoff to calculate a ubiquity score of each gene [53]. Then, we prepared the precursorMets list which included all metabolites involved in the 'BIOMASS_maintenance' reaction and the confidence score of all reactions in Recon3D. We obtained the draft reconstruction using these input parameters and employing the *pymCADRE* algorithm.

iMAT and *tINIT*: python version of both *iMAT* and *tINIT* are integrated into the *troppo* (v0.0.7, <https://github.com/BioSystemsUM/troppo>). Similar to the *pymCADRE* protocol, we set the 30th quantile of normalized expression data as our gene expression cutoff. Then we took median values among all samples as gene expression values. All values below the cutoff were converted to 0, while values over the cutoff were log2 transformed. Using the gene expression values, we obtained the reaction scores in *troppo* [54].

CORDA: *CORDA* (v0.17, <https://github.com/resendislab/corda>) is also a reconstruction tool in python. We used the same reaction scores as *iMAT* and *tINIT* and recalculated them at three expression levels, as required in *CORDA* [55]. The target metabolites required by *CORDA* were the same as those on the *pymCADRE* precursorMets list.

We used *pymCADRE*, *iMAT*, *tINIT* and *CORDA* to get four draft reconstructions, that were used for generating the consensus reconstruction.

Generation of consensus reconstruction

We identified overlapping reactions, genes and metabolites for the draft reconstructions, and built a consensus reconstruction which included all reactions from the four draft reconstructions except reactions unique to the draft reconstructions of *tINIT*. The draft reconstruction generated by *tINIT* contained the most reactions. After running FASTCC, the output

of tINIT draft reconstruction contained the greatest number of unique metabolites and genes among the four reconstructions, implying a higher level of uniqueness of the tINIT reconstruction. Therefore, we excluded reactions unique to tINIT and merged other reactions in the four draft reconstructions to build a consensus reconstruction for the following analyses.

Metabolic task analysis for specificity testing

We tested the specificity of our consensus reconstruction using the information from 229 reported metabolic functions known to be feasible for human colonocytes as well as general human cells (Table F in [S1 Data](#)). In brief, the reconstruction was closed by setting lower boundaries of both exchange and sink reactions to 0. Then for each metabolic task, reactants would be available for the reconstruction by setting the corresponding exchange reactions or sink reactions to -1. We added a sink reaction for the product of each metabolic task and set it as the objective. We ran `model.optimize` function in COBRAPy [\[56\]](#) to optimize the sink reaction to check if it could achieve a flux value over 0.

Curating the transport reactions module

To allow our human colonic epithelial cell reconstruction to connect and interact with the gut microbiome, we built a lumen compartment containing transport reactions which enable the exchange of metabolites between colonic epithelial cells and the gut microbiome. We collected genes associated with transport functions from the Human Protein Atlas (www.protein-atlas.org) [\[23\]](#) and also retained the genes which were part of the consensus reconstruction (Table G in [S1 Data](#)). Then, we searched metabolic reactions related to these genes in Uniport [\[25\]](#), after which metabolites from these reactions were extracted. Meanwhile, we also extract metabolites from a published human membrane transporter module [\[26\]](#), and colon transport reactions of the human whole-body model [\[17\]](#). After curating a list of metabolites from sources described above, we identified those that overlapped with the consensus reconstruction. Finally, transport reactions associated with these metabolites were added to the lumen compartment to allow metabolite exchanges with gut microbiota.

Testing basic properties of reconstruction

The quality of our reconstruction was checked with a series of tests implemented in the COBRA Toolbox [\[57\]](#), including leak tests and sanity checks [\[17\]](#). During the tests, all demand, sink and exchange reactions in our reconstruction were closed, and then the closed reconstruction was checked for (1) whether it could produce any exchange metabolites with or without a demand reaction for each metabolite; (2) whether it could produce energy from water or oxygen; (3) whether it could produce any metabolites with a reversed ATP demand reaction; (4) whether it could achieve flux consistency – dead ends in the reconstruction were detected and excluded with FVA [\[32\]](#).

Differentiated Caco-2 cell lines and metabolomics analysis

Caco-2 cells were purchased from American Type Culture Collection (Manassas, VA) and cultured in a 37°C humidified incubator with 5% CO₂ utilizing T-75 flasks (FB012937, Fisherbrand), with Dulbecco's Modified Eagle Medium (DMEM) (10–013-CV, Corning, supplemented with 10% fetal bovine serum (FBS) (S11150, R&D). To induce differentiation, the medium was replaced every 2–3 days. Cells were passaged using trypsin (25–03-CI, Corning). At the end of the experimental timeline, culturing medium of the Caco-2 cells and fresh DMEM + FBS was collected for targeted metabolomics analysis of SCFAs (butyrate, acetate and propionate) and 20 amino acids ([Table 2](#)). The concentration of SCFAs in samples was detected using a reported liquid chromatography with tandem mass spectrometry (LC-MS-MS) method [\[58\]](#) in the Bindley Bioscience Center at Purdue University. Raw data of metabolomics analysis can be found in [S1 Table](#).

Analysis of IBD patient-derived samples

We collected scRNAseq data of human colon epithelium from two studies: a CD study [\[34\]](#) and a UC study [\[35\]](#). They both contained more than three samples each in the IBD groups and healthy control groups. Colonocyte gene expression

matrices from IBD samples and healthy samples, for both CD and UC studies, were extracted using the Seurat package in R [59]. Then, using iMAT, we integrated gene expression data of each sample with our iColonEpithelium to build context-specific reconstructions of all samples. We ran FVA on each context-specific reconstruction and performed student's t-test ($\alpha < 0.05$) on the maximum fluxes between IBD and healthy control groups. This analysis led to the identification of fluxes with significant differences across UC and CD vs healthy control groups. Genes associated with these differential reactions were also collected.

In addition to FVA, we also employed the ACHR flux sampling function in the COBRApy with a thinning factor of 1000. This provided us with random samples of steady-state fluxes with the allowable solution space of each context-specific reconstruction. Solutions from flux sampling were used to compare the flux distributions between IBD and healthy control groups.

We performed single gene deletion simulation on all context-specific reconstructions. In brief, we knocked out one gene at a time, and then ran FVA to obtain the maximum flux of specific reactions. Then according to a method from a published study [60], we calculated the ratio of altered maximum fluxes caused by a single gene knockout in the IBD and healthy control groups, respectively. Finally, ratios between the IBD and healthy groups were compared. In the CD study, the gene *PCYT2* was considered as an outlier and removed from the volcano plot, original plot containing *PCYT2* was in [S1Fig](#).

Integrated model to study host-microbiome interactions

We prepared a metabolic model of microbial communities based on MICOM [38], which includes 36 gut microbiota taxa (Table J in [S1 Data](#)). Then the MICOM model was connected to the iColonEpithelium reconstruction with the shared lumen compartment. After applying the average European diet medium [61] to the MICOM model, we optimized the host biomass maintenance reaction in the integrated model with the cooperative tradeoff function in MICOM, to explore metabolite exchanges with between the gut microbiome and human colonocytes.

Supporting information

S1 Data. Detailed analysis of iColonEpithelium reconstruction (Microsoft Excel Workbook: Tables A - L).
(XLSX)

S2 Data. MEMOTE results.
(PDF)

S1 Table. Raw data of metabolomics analysis.
(XLSX)

S1 Fig. Volcano plot with *PCYT2* representation.
(TIFF)

Acknowledgments

We thank the EMBRIO Institute, Purdue University, for providing laboratory space for Baloni lab members that facilitated this work.

Author contributions

Conceptualization: Priyanka Baloni.

Data curation: Boyu Jiang.

Formal analysis: Boyu Jiang, Nick Quinn-Bohmann, Christian Diener, Priyanka Baloni.

Funding acquisition: Sean M Gibbons.

Investigation: Boyu Jiang, Nick Quinn-Bohmann, Vignesh Bose Nathan, Priyanka Baloni.

Methodology: Boyu Jiang, Priyanka Baloni.

Resources: Lavanya Reddivari, Sean M Gibbons, Priyanka Baloni.

Supervision: Sean M Gibbons, Priyanka Baloni.

Validation: Vignesh Bose Nathan, Yu Han-Hallett, Lavanya Reddivari, Priyanka Baloni.

Writing – original draft: Boyu Jiang, Priyanka Baloni.

Writing – review & editing: Nick Quinn-Bohmann, Christian Diener, Vignesh Bose Nathan, Yu Han-Hallett, Lavanya Reddivari, Sean M Gibbons.

References

- Dupont HL, Jiang Z-D, Dupont AW, Utay NS. The intestinal microbiome in human health and disease. *Trans Am Clin Climatol Assoc.* 2020;131:178–97. PMID: [32675857](https://pubmed.ncbi.nlm.nih.gov/32675857/)
- Odenwald MA, Turner JR. The intestinal epithelial barrier: a therapeutic target?. *Nat Rev Gastroenterol Hepatol.* 2017;14(1):9–21. <https://doi.org/10.1038/nrgastro.2016.169> PMID: [27848962](https://pubmed.ncbi.nlm.nih.gov/27848962/)
- Groschwitz KR, Hogan SP. Intestinal barrier function: molecular regulation and disease pathogenesis. *J Allergy Clin Immunol.* 2009;124(1):3–20; quiz 21–2. <https://doi.org/10.1016/j.jaci.2009.05.038> PMID: [19560575](https://pubmed.ncbi.nlm.nih.gov/19560575/)
- Martini E, Krug SM, Siegmund B, Neurath MF, Becker C. Mend Your Fences: The Epithelial Barrier and its Relationship With Mucosal Immunity in Inflammatory Bowel Disease. *Cell Mol Gastroenterol Hepatol.* 2017;4(1):33–46. <https://doi.org/10.1016/j.jcmgh.2017.03.007> PMID: [28560287](https://pubmed.ncbi.nlm.nih.gov/28560287/)
- Pellegrini C, Fornai M, D'Antongiovanni V, Antonioli L, Bernardini N, Derkinderen P. The intestinal barrier in disorders of the central nervous system. *Lancet Gastroenterol Hepatol.* 2023;8(1):66–80. [https://doi.org/10.1016/S2468-1253\(22\)00241-2](https://doi.org/10.1016/S2468-1253(22)00241-2) PMID: [36334596](https://pubmed.ncbi.nlm.nih.gov/36334596/)
- Chelakkot C, Ghim J, Ryu SH. Mechanisms regulating intestinal barrier integrity and its pathological implications. *Exp Mol Med.* 2018;50(8):1–9. <https://doi.org/10.1038/s12276-018-0126-x> PMID: [30115904](https://pubmed.ncbi.nlm.nih.gov/30115904/)
- Litvak Y, Byndloss MX, Bäumlér AJ. Colonocyte metabolism shapes the gut microbiota. *Science.* 2018;362(6418):eaat9076. <https://doi.org/10.1126/science.aat9076> PMID: [30498100](https://pubmed.ncbi.nlm.nih.gov/30498100/)
- Taylor SJ, Winter MG, Gillis CC, Silva LAD, Dobbins AL, Muramatsu MK, et al. Colonocyte-derived lactate promotes *E. coli* fitness in the context of inflammation-associated gut microbiota dysbiosis. *Microbiome.* 2022;10(1):200. <https://doi.org/10.1186/s40168-022-01389-7> PMID: [36434690](https://pubmed.ncbi.nlm.nih.gov/36434690/)
- Diener C, Dai CL, Wilmanski T, Baloni P, Smith B, Rappaport N, et al. Genome-microbiome interplay provides insight into the determinants of the human blood metabolome. *Nat Metab.* 2022;4(11):1560–72. <https://doi.org/10.1038/s42255-022-00670-1> PMID: [36357685](https://pubmed.ncbi.nlm.nih.gov/36357685/)
- Rath E, Haller D. Intestinal epithelial cell metabolism at the interface of microbial dysbiosis and tissue injury. *Mucosal Immunol.* 2022;15(4):595–604. <https://doi.org/10.1038/s41385-022-00514-x> PMID: [35534699](https://pubmed.ncbi.nlm.nih.gov/35534699/)
- Fang X, Lloyd CJ, Palsson BO. Reconstructing organisms in silico: genome-scale models and their emerging applications. *Nat Rev Microbiol.* 2020;18(12):731–43. <https://doi.org/10.1038/s41579-020-00440-4> PMID: [32958892](https://pubmed.ncbi.nlm.nih.gov/32958892/)
- Passi A, Tibocha-Bonilla JD, Kumar M, Tec-Campos D, Zengler K, Zuniga C. Genome-Scale Metabolic Modeling Enables In-Depth Understanding of Big Data. *Metabolites.* 2021;12(1):14. <https://doi.org/10.3390/metabo12010014> PMID: [35050136](https://pubmed.ncbi.nlm.nih.gov/35050136/)
- Orth JD, Thiele I, Palsson BØ. What is flux balance analysis?. *Nat Biotechnol.* 2010;28(3):245–8. <https://doi.org/10.1038/nbt.1614> PMID: [20212490](https://pubmed.ncbi.nlm.nih.gov/20212490/)
- Wang Q, Chen X, Yang Y, Zhao X. Genome-scale in silico aided metabolic analysis and flux comparisons of *Escherichia coli* to improve succinate production. *Appl Microbiol Biotechnol.* 2006;73(4):887–94. <https://doi.org/10.1007/s00253-006-0535-y> PMID: [16927085](https://pubmed.ncbi.nlm.nih.gov/16927085/)
- Quinn-Bohmann N, Wilmanski T, Sarmiento KR, Levy L, Lampe JW, Gurry T, et al. Microbial community-scale metabolic modelling predicts personalized short-chain fatty acid production profiles in the human gut. *Nat Microbiol.* 2024;9(7):1700–12. <https://doi.org/10.1038/s41564-024-01728-4> PMID: [38914826](https://pubmed.ncbi.nlm.nih.gov/38914826/)
- Sen P, Orešič M. Metabolic Modeling of Human Gut Microbiota on a Genome Scale: An Overview. *Metabolites.* 2019;9(2):22. <https://doi.org/10.3390/metabo9020022> PMID: [30695998](https://pubmed.ncbi.nlm.nih.gov/30695998/)
- Thiele I, Sahoo S, Heinken A, Hertel J, Heirendt L, Aurich MK, et al. Personalized whole-body models integrate metabolism, physiology, and the gut microbiome. *Mol Syst Biol.* 2020;16(5):e8982. <https://doi.org/10.1525/msb.20198982> PMID: [32463598](https://pubmed.ncbi.nlm.nih.gov/32463598/)
- van der Ark KCH, van Heck RGA, Martins Dos Santos VAP, Belzer C, de Vos WM. More than just a gut feeling: constraint-based genome-scale metabolic models for predicting functions of human intestinal microbes. *Microbiome.* 2017;5(1):78. <https://doi.org/10.1186/s40168-017-0299-x> PMID: [28705224](https://pubmed.ncbi.nlm.nih.gov/28705224/)

19. Brunk E, Sahoo S, Zielinski DC, Altunkaya A, Dräger A, Mih N, et al. Recon3D enables a three-dimensional view of gene variation in human metabolism. *Nat Biotechnol.* 2018;36(3):272–81. <https://doi.org/10.1038/nbt.4072> PMID: 29457794
20. Schwärzler J, Mayr L, Grabherr F, Tilg H, Adolph TE. Epithelial metabolism as a rheostat for intestinal inflammation and malignancy. *Trends Cell Biol.* 2024;34(11):913–27. <https://doi.org/10.1016/j.tcb.2024.01.004> PMID: 38341347
21. Blachier F, Davila AM, Benamouzig R, Tome D. Channelling of arginine in NO and polyamine pathways in colonocytes and consequences. *Front Biosci (Landmark Ed).* 2011;16(4):1331–43. <https://doi.org/10.2741/3792> PMID: 21196235
22. Phan CT, Tso P. Intestinal lipid absorption and transport. *Front Biosci.* 2001;6:D299–319. <https://doi.org/10.2741/phan> PMID: 11229876
23. Uhlen M, Karlsson MJ, Zhong W, Tebani A, Pou C, Mikes J, et al. A genome-wide transcriptomic analysis of protein-coding genes in human blood cells. *Science.* 2019;366(6472):eaax9198. <https://doi.org/10.1126/science.aax9198> PMID: 31857451
24. Bansal P, Morgat A, Axelsen KB, Muthukrishnan V, Coudert E, Aimo L, et al. Rhea, the reaction knowledgebase in 2022. *Nucleic Acids Res.* 2022;50(D1):D693–700. <https://doi.org/10.1093/nar/gkab1016> PMID: 34755880
25. Bateman A, Martin MJ, Orchard S, Magrane M, Ahmad S, Alpi E, et al. UniProt: the Universal Protein Knowledgebase in 2023. *Nucleic Acids Res.* 2023;51:D523–D531. [doi:10.1093/nar/gkac1052](https://doi.org/10.1093/nar/gkac1052)
26. Sahoo S, Aurich MK, Jonsson JJ, Thiele I. Membrane transporters in a human genome-scale metabolic knowledgebase and their implications for disease. *Front Physiol.* 2014;5:91. <https://doi.org/10.3389/fphys.2014.00091> PMID: 24653705
27. Leinonen R, Akhtar R, Birney E, Bower L, Cerdeno-Tárraga A, Cheng Y, et al. The European Nucleotide Archive. *Nucleic Acids Res.* 2011;39(Database issue):D28–31. <https://doi.org/10.1093/nar/gkq967> PMID: 20972220
28. Fedi A, Vitale C, Ponschin G, Ayehunie S, Fato M, Scaglione S. In vitro models replicating the human intestinal epithelium for absorption and metabolism studies: A systematic review. *J Control Release.* 2021;335:247–68. <https://doi.org/10.1016/j.jconrel.2021.05.028> PMID: 34033859
29. Alaqbi SS, Burke L, Guterman I, Green C, West K, Palacios-Gallego R, et al. Increased mitochondrial proline metabolism sustains proliferation and survival of colorectal cancer cells. *PLoS One.* 2022;17(2):e0262364. <https://doi.org/10.1371/journal.pone.0262364> PMID: 35130302
30. Stein J, Zores M, Schröder O. Short-chain fatty acid (SCFA) uptake into Caco-2 cells by a pH-dependent and carrier mediated transport mechanism. *Eur J Nutr.* 2000;39(3):121–5. <https://doi.org/10.1007/s003940070028> PMID: 10918994
31. Lee DY, Yun SH, Lee SY, Lee J, Jr Mariano E, Joo S-T, et al. Analysis of commercial fetal bovine serum (FBS) and its substitutes in the development of cultured meat. *Food Res Int.* 2023;174(Pt 1):113617. <https://doi.org/10.1016/j.foodres.2023.113617> PMID: 37986472
32. Thiele I, Swainston N, Fleming RMT, Hoppe A, Sahoo S, Aurich MK, et al. A community-driven global reconstruction of human metabolism. *Nat Biotechnol.* 2013;31(5):419–25. <https://doi.org/10.1038/nbt.2488> PMID: 23455439
33. Lieven C, Beber ME, Olivier BG, Bergmann FT, Ataman M, Babaei P, et al. MEMOTE for standardized genome-scale metabolic model testing. *Nat Biotechnol.* 2020;38(3):272–6. <https://doi.org/10.1038/s41587-020-0446-y> PMID: 32123384
34. Kanke M, Kennedy Ng MM, Connelly S, Singh M, Schaner M, Shanahan MT, et al. Single-Cell Analysis Reveals Unexpected Cellular Changes and Transposon Expression Signatures in the Colonic Epithelium of Treatment-Naïve Adult Crohn's Disease Patients. *Cell Mol Gastroenterol Hepatol.* 2022;13(6):1717–40. <https://doi.org/10.1016/j.jcmgh.2022.02.005> PMID: 35158099
35. Smillie CS, Biton M, Ordovas-Montanes J, Sullivan KM, Burgin G, Graham DB, et al. Intra- and Inter-cellular Rewiring of the Human Colon during Ulcerative Colitis. *Cell.* 2019;178(3):714–730.e22. <https://doi.org/10.1016/j.cell.2019.06.029> PMID: 31348891
36. Zur H, Ruppin E, Shlomi T. iMAT: an integrative metabolic analysis tool. *Bioinformatics.* 2010;26(24):3140–2. <https://doi.org/10.1093/bioinformatics/btq602> PMID: 21081510
37. Proffitt C, Bidkhorji G, Lee S, Tebani A, Mardinoglu A, Uhlen M, et al. Genome-scale metabolic modelling of the human gut microbiome reveals changes in the glyoxylate and dicarboxylate metabolism in metabolic disorders. *iScience.* 2022;25(7):104513. <https://doi.org/10.1016/j.isci.2022.104513> PMID: 35754734
38. Diener C, Gibbons SM, Resendis-Antonio O. MICOM: Metagenome-Scale Modeling To Infer Metabolic Interactions in the Gut Microbiota. *mSystems.* 2020;5(1):e00606–19. <https://doi.org/10.1128/mSystems.00606-19> PMID: 31964767
39. Kong S, Zhang YH, Zhang W. Regulation of Intestinal Epithelial Cells Properties and Functions by Amino Acids. *Biomed Res Int.* 2018;2018:2819154. <https://doi.org/10.1155/2018/2819154> PMID: 29854738
40. den Besten G, van Eunen K, Groen AK, Venema K, Reijngoud D-J, Bakker BM. The role of short-chain fatty acids in the interplay between diet, gut microbiota, and host energy metabolism. *J Lipid Res.* 2013;54(9):2325–40. <https://doi.org/10.1194/jlr.R036012> PMID: 23821742
41. Piotrowska M, Binienda A, Fichna J. The role of fatty acids in Crohn's disease pathophysiology - An overview. *Mol Cell Endocrinol.* 2021;538:111448. <https://doi.org/10.1016/j.mce.2021.111448> PMID: 34480991
42. Crittenden S, Cheyne A, Adams A, Forster T, Robb CT, Felton J, et al. Purine metabolism controls innate lymphoid cell function and protects against intestinal injury. *Immunol Cell Biol.* 2018;96(10):1049–59. <https://doi.org/10.1111/imcb.12167> PMID: 29758102
43. Wang S, van Schooten F-J, Jin H, Jonkers D, Godschalk R. The Involvement of Intestinal Tryptophan Metabolism in Inflammatory Bowel Disease Identified by a Meta-Analysis of the Transcriptome and a Systematic Review of the Metabolome. *Nutrients.* 2023;15(13):2886. <https://doi.org/10.3390/nu15132886> PMID: 37447212
44. Bodriagina E, Nabatov A, Gainullina G. P211 Relationship between the concentrations of free sulphates and 5-hydroxyindoleacetic acid (5-HIAA) in urine for IBD patients. *Journal of Crohn's and Colitis.* 2019;13(Supplement_1):S200–S200. <https://doi.org/10.1093/ecco-jcc/jyy222.335>

45. Xue X, Miao Y, Wei Z. Nicotinamide adenine dinucleotide metabolism: driving or counterbalancing inflammatory bowel disease?. *FEBS Lett.* 2023;597(9):1179–92. <https://doi.org/10.1002/1873-3468.14528> PMID: [36310388](https://pubmed.ncbi.nlm.nih.gov/36310388/)
46. Zong C, Nie X, Zhang D, Ji Q, Qin Y, Wang L, et al. Up regulation of glyoxylate reductase/hydroxypyruvate reductase (GRHPR) is associated with intestinal epithelial cells apoptosis in TNBS-induced experimental colitis. *Pathol Res Pract.* 2016;212(5):365–71. <https://doi.org/10.1016/j.prp.2015.09.019> PMID: [26997491](https://pubmed.ncbi.nlm.nih.gov/26997491/)
47. Becker HM, Seidler UE. Bicarbonate secretion and acid/base sensing by the intestine. *Pflugers Arch.* 2024;476(4):593–610. <https://doi.org/10.1007/s00424-024-02914-3> PMID: [38374228](https://pubmed.ncbi.nlm.nih.gov/38374228/)
48. Zeng X, Xing X, Gupta M, Keber FC, Lopez JG, Lee YC, et al. Gut bacterial nutrient preferences quantified in vivo. *Cell.* 2022; 185(18):3441–56. e19. <https://doi.org/10.1016/j.cell.2022.07.020>
49. Parada Venegas D, De la Fuente MK, Landskron G, González MJ, Quera R, Dijkstra G, et al. Short Chain Fatty Acids (SCFAs)-Mediated Gut Epithelial and Immune Regulation and Its Relevance for Inflammatory Bowel Diseases. *Front Immunol.* 2019;10:277. <https://doi.org/10.3389/fimmu.2019.00277> PMID: [30915065](https://pubmed.ncbi.nlm.nih.gov/30915065/)
50. Borzou P, Ghaisari J, Izadi I, Eshraghi Y, Gheisari Y. A novel strategy for dynamic modeling of genome-scale interaction networks. *Bioinformatics.* 2023;39(2):btad079. <https://doi.org/10.1093/bioinformatics/btad079> PMID: [36825834](https://pubmed.ncbi.nlm.nih.gov/36825834/)
51. Borisov N, Sorokin M, Zolotovskaya M, Borisov C, Buzdin A. Shambhala-2: A Protocol for Uniformly Shaped Harmonization of Gene Expression Profiles of Various Formats. *Curr Protoc.* 2022;2(5):e444. <https://doi.org/10.1002/cpz1.444> PMID: [35617464](https://pubmed.ncbi.nlm.nih.gov/35617464/)
52. Leonidou N, Renz A, Mostolizadeh R, Dräger A. New workflow predicts drug targets against SARS-CoV-2 via metabolic changes in infected cells. *PLoS Comput Biol.* 2023;19(3):e1010903. <https://doi.org/10.1371/journal.pcbi.1010903> PMID: [36952396](https://pubmed.ncbi.nlm.nih.gov/36952396/)
53. Wang Y, Eddy JA, Price ND. Reconstruction of genome-scale metabolic models for 126 human tissues using mCADRE. *BMC Syst Biol.* 2012;6:153. <https://doi.org/10.1186/1752-0509-6-153> PMID: [23234303](https://pubmed.ncbi.nlm.nih.gov/23234303/)
54. Ferreira J, Vieira V, Gomes J, Correia S, Rocha M. Troppo - A Python Framework for the Reconstruction of Context-Specific Metabolic Models. *Advances in Intelligent Systems and Computing.* Springer International Publishing. 2019;146–53. https://doi.org/10.1007/978-3-030-23873-5_18
55. Schultz A, Qutub AA. Reconstruction of Tissue-Specific Metabolic Networks Using CORDA. *PLoS Comput Biol.* 2016;12(3):e1004808. <https://doi.org/10.1371/journal.pcbi.1004808> PMID: [26942765](https://pubmed.ncbi.nlm.nih.gov/26942765/)
56. Ebrahim A, Lerman JA, Palsson BO, Hyduke DR. COBRApy: COntstraints-Based Reconstruction and Analysis for Python. *BMC Syst Biol.* 2013;7:74. <https://doi.org/10.1186/1752-0509-7-74> PMID: [23927696](https://pubmed.ncbi.nlm.nih.gov/23927696/)
57. Heirendt L, Arreckx S, Pfau T, Mendoza SN, Richelle A, Heinken A, et al. Creation and analysis of biochemical constraint-based models using the COBRA Toolbox v.3.0. *Nat Protoc.* 2019;14(3):639–702. <https://doi.org/10.1038/s41596-018-0098-2> PMID: [30787451](https://pubmed.ncbi.nlm.nih.gov/30787451/)
58. Chan JCY, Kioh DYQ, Yap GC, Lee BW, Chan ECY. A novel LCMSMS method for quantitative measurement of short-chain fatty acids in human stool derivatized with 12C- and 13C-labelled aniline. *J Pharm Biomed Anal.* 2017;138:43–53. <https://doi.org/10.1016/j.jpba.2017.01.044> PMID: [28178633](https://pubmed.ncbi.nlm.nih.gov/28178633/)
59. Hao Y, Hao S, Andersen-Nissen E, Mauck WM 3rd, Zheng S, Butler A, et al. Integrated analysis of multimodal single-cell data. *Cell.* 2021;184(13):3573–3587. e29. <https://doi.org/10.1016/j.cell.2021.04.048> PMID: [34062119](https://pubmed.ncbi.nlm.nih.gov/34062119/)
60. Lewis JE, Forshaw TE, Boothman DA, Furdui CM, Kemp ML. Personalized Genome-Scale Metabolic Models Identify Targets of Redox Metabolism in Radiation-Resistant Tumors. *Cell Syst.* 2021;12(1):68–81. e11. <https://doi.org/10.1016/j.cels.2020.12.001> PMID: [33476554](https://pubmed.ncbi.nlm.nih.gov/33476554/)
61. Noronha A, Modamio J, Jarosz Y, Guerard E, Sompairac N, Preciat G, et al. The Virtual Metabolic Human database: integrating human and gut microbiome metabolism with nutrition and disease. *Nucleic Acids Res.* 2019;47(D1):D614–24. <https://doi.org/10.1093/nar/gky992> PMID: [30371894](https://pubmed.ncbi.nlm.nih.gov/30371894/)